JOURNAL OF THERMOPHYSICS AND HEAT TRANSFER
Vol. 13, No. 2, April–June 1999

Kinetics of Free Radicals Behind Strong Shock Waves

Djameel Ramjaun,* Michel Dumitrescu,† and Raymond Brun‡
Université de Provence, 13453 Marseille CEDEX 13, France

A spectroscopic study of the spontaneous emission of free radicals behind strong shocks propagating in the simulated atmospheres of Titan and Mars and in pure CO gas has been carried out in the hypersonic facility of Marseille. A streak camera has been used to obtain time-resolved spectra of the $\Delta v = 0$ sequence of the $B^2\Sigma^+ \leftrightarrow X^2\Sigma^+$ electronic transition of CN, which is the main emitter in these mixtures. The Swan system of C_2 has also been measured in CO gas. The effect of different initial test gas pressures in the shock tube on the emission of CN in the Titan mixture has been investigated. The comparison between experimental and synthetic spectra shows very high nonequilibrium phenomena in the shock layer. Evidence of non-Boltzmann distribution of the vibrational population of CN has been observed, particularly in high initial pressure conditions.

Nomenclature

A = constant for a vibrational sequence
c = speed of light
F = rotational energy
G = vibrational energy
h = Planck constant
J' = excited rotational level
k = Boltzmann constant
N = number density of molecules in a given state
N_0 = total number density of molecules
n' = excited electronic level
p_1 = initial test gas pressure
Q_{tot} = total partition function
T_{elec} = electronic temperature
T_{rot} = rotational temperature
T_{vib} = vibrational temperature
V = shock speed
v' = excited vibrational level
x = distance from maximum emission intensity
ν_e' = electronic energy term

Introduction

THE entry velocity of space vehicles in the atmospheres of Titan and Mars may be greater than 6 km/s. In such conditions, high-enthalpy flows are generated around these vehicles, and because of the high temperature and low pressure, nonequilibrium effects occur behind the shock wave. Also, the temperature is high enough to dissociate the molecular constituents of the gas and to ionize them. Thermal nonequilibrium leads to strong radiative heating that constitutes an important part of the total heat flux. Therefore, to properly design the heat shields of these space vehicles, a considerable amount of work is necessary to numerically simulate high-temperature flows accurately. Experiments behind strong shock waves enable an evaluation of physical constants and provide a basis for improving the thermochemical models used in these numerical simulations.

Received July 8, 1998; revision received Nov. 2, 1998; accepted for publication Nov. 2, 1998.

*Ph.D. Candidate, Institut Universitaire des Systèmes Thermiques Industriels. Member AIAA.

†Research Engineer, Institut Universitaire des Systèmes Thermiques Industriels. Senior Member AIAA.

‡Professor Emeritus, Institut Universitaire des Systèmes Thermiques Industriels.

A large number of experiments carried out on the radiative behavior behind shock waves can be found in the literature. In the Avco–Everett Research Laboratory,[1] investigations were made in nitrogen and air using spectrographs, photomultipliers, and rotating drum cameras as measuring tools. Park et al.[2] used high-speed films to measure spectra behind shock waves in a simulated Titan atmosphere in the Stanford University shock-tube facility. In the Marseille facility (TCM2), a spectroscopic study of CN emission in the same mixture, which required the use of a special optical fiber bundle equipped with three slits, was carried out by Labracherie.[3] The bundle, placed at the end of a monochromator, enabled the capturing of the emission at three different wavelengths, the intensities of which were then recorded by photomultipliers. From these results, the evolution of the vibrational temperature behind the shock was deduced and compared with a numerical computation by Baillon et al.[4] More recently, at Chiba University, a streak camera coupled with a monochromator was used by Morioka et al.[5] to obtain time-resolved spectra of N_2^+ behind shock waves in air.

In this work, an imaging spectroscopy technique similar to that of Morioka et al. was used. Simultaneous wavelength–intensity–time information obtained thereby provided details of the emission of CN occurring within 16 μs behind shock waves in the simulated atmospheres of Titan and Mars. The composition of the Titan atmosphere[6] was chosen to be 92% N_2–3% CH_4–5% Ar, and that of Mars[7] to be 70% CO_2–30% N_2. The proportion of N_2 in the second mixture was higher than usual because previous spectroscopic measurement of CN emission in 97% CO_2–3% N_2 gave a level of signal that was too low to be properly exploited by the present measuring system. The measurement of the Swan bands of C_2 in the CO_2–N_2 mixture also gave unsatisfactory results. Emission from these bands were recorded behind shocks in pure CO gas.

Calculation of Flowfield Parameters

Using a code developed in Ref. 8, a numerical calculation of the flowfield variables and species concentration behind a strong normal shock was carried out. The code used a three-temperature model; i.e., the translational, vibrational, and electronic temperatures are not necessarily the same. The governing equations for mass, momentum, and total energy of the gas, as well as vibrational and electronic energy, were solved behind the shock wave using a Runge–Kutta scheme. Twenty species were taken into account: H_2, N_2, C_2, CN, NH, CH, CH_2, CH_3, CH_4, H, N, C, Ar, H^+, N^+, C^+, Ar^+, CN^+, N_2^+, and e^- in a scheme of 24 reactions. Figure 1 shows the evolution of temperatures behind a shock wave in a 97% N_2–3%

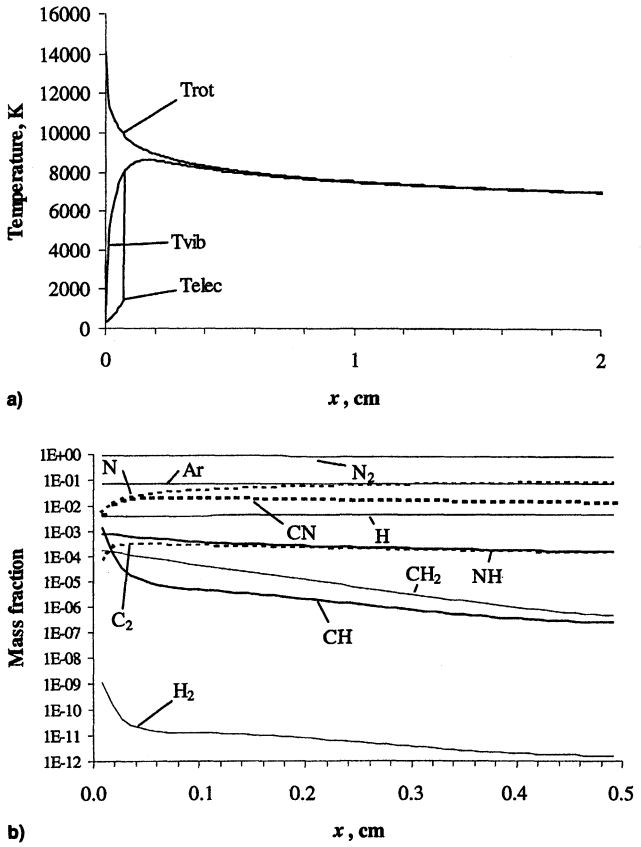

Fig. 1 Thermodynamic state variables as functions of distance behind a shock in the CH_4-N_2-Ar mixture for p_1 = 2.19 mb and V = 5800 m/s: a) temperatures and b) species mass fractions.

CH_4–5% Ar mixture, computed with the following initial conditions: pressure = 2 mb, temperature = 300 K, and shock speed = 5560 m/s.

The calculation of the thermophysical variables, species concentrations, and temperatures in the CO_2-N_2 mixture was done by Mazoué.[9] Detailed information on the chemical reaction rates may be found therein. The calculation assumes a chemical scheme proposed by Park et al.,[7] involving 19 chemical reactions with the following 10 species: CO_2, CO, C, C_2, CN, O_2, O, N_2, N, and NO; the presence of ionized species being neglected because of their very small configurations. The numerical calculation is similar to that of Ref. 8. However, the vibrational energy of the molecules CO_2, CO, and N_2 are calculated separately, so that their corresponding vibrational temperatures may be determined.

To compare with the experiments carried out in pure CO gas, a numerical code has been written that computes the flow parameters variables behind a shock wave using a scheme of five reactions and five species: CO, C_2, O_2, C, and O. Rate constants for CO were taken from Hanson[10] and the vibrational relaxation rate of CO is given by Appleton et al.[11]

Radiation

The observation of the spontaneous emission behind the shock waves, for the CN radical, was focused on the near ultraviolet region of the $B^2\Sigma^+ \leftrightarrow X^2\Sigma^+$ electronic transition, more precisely on the $\Delta v = 0$ sequence of this transition, which is known to have the strongest intensity. For the C_2 radical, the $\Delta v = 0$ and $\Delta v = +1$ bands of the $A^3\Pi_g \leftrightarrow X^3\Pi_u$ electronic transition (Swan bands) were recorded. These electronic transitions have been studied during the past decades and molecular constants necessary for the calculation of the corresponding synthetic spectra can be found in the literature.[12–15]

Spectrum Calculation

For the vibrational transitions of the CN violet system, the Frank–Condon factor was taken from Spindler,[16] and spectroscopic constants were taken from Rehfuss et al.[13] and Engleman.[12] The intensity of a rotational line belonging to an electronic transition is proportional to the number density of excited molecules, $N(n', v', J')$. Assuming a Boltzmann distribution, the number of excited molecules is classically written in terms of the respective temperatures as

$$N(n', v', J') = N_0 \frac{(2J' + 1)}{Q_{\text{tot}}} \times \exp\left\{-\frac{hc}{k}\left[\frac{F(n', v', J')}{T_{\text{rot}}} + \frac{G(n', v')}{T_{\text{vib}}} + \frac{\nu'_e}{T_{\text{elec}}}\right]\right\} \quad (1)$$

Line broadening as a result of pressure and Doppler effect is applied to the vibrational and rotational lines calculated by convoluting them with a Gaussian and Lorentzian function. However, an approximation assuming a Voigt profile, taken from Arnold et al.,[17] is used to decrease the computational time of the spectrum. Convolution caused by slit functions of the measuring system is then applied to obtain the final synthetic spectrum.

Vibrational Population Calculation

In the experiments presented next, only the relative intensity of the lines in the $\Delta v = 0$ band of the CN violet system was of interest; thus, all factors that are constant for the observed spectral sequence may be omitted, e.g., the electronic transition moment term and the total partition function of the molecule. To estimate the vibrational population distribution, one may write the number density of the $B^2\Sigma^+$ molecules of CN as a product of a Boltzmann factor and a vibrational population factor $N(v')$, assuming that the rotational temperature is in equilibrium with the translational temperature:

$$N(n', v', J') = A(2J' + 1)\exp\left[-\frac{hc}{k}\frac{F(n', v', J')}{T_{\text{rot}}}\right] \times N(v') \quad (2)$$

An iterative method is used to estimate the vibrational population relative to the level $v = 0$. The vibrational population on a given level is adjusted so that the corresponding peak intensity on the calculated spectrum is equal to the one on the experimental spectrum. This process is repeated on each vibrational sequence; at each iteration the spectrum is recalculated to take into account the changes introduced. The calculation is carried out up to $v = 8$ and the iteration is stopped when the greatest difference between two successive calculated vibrational populations is less than 1%. Beyond $v = 8$, this procedure is not valid because of overlapping of the vibrational bands. When possible, a linear regression is applied to the population density data to evaluate the vibrational temperature. The rotational temperature used in these calculations was taken from the theoretical computations.[8,9] Numerical experiments done to evaluate the error induced by the rotational temperature on the calculation of the vibrational temperature show that an error of 1000 K in the rotational temperature results in a variation of 250 K in the vibrational temperature.

Experiment

TCM2 Facility

The TCM2 hypersonic facility[18] is a free-piston shock tunnel producing shock speeds in the range of 2–6 km/s (Fig. 2). Strong shock waves can be generated in the shock tube after a preliminary compression of the driver gas (helium) by the piston, which had a mass of 35 kg for the shots presented in this work. The compression chamber and the shock tube are

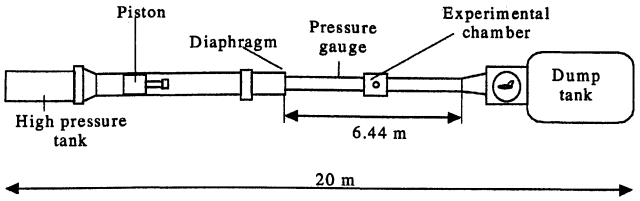

Fig. 2 Schematic of the TCM2 hypersonic facility.

separated by a steel diaphragm calibrated to burst at ~200 bar. During these experiments, the pressure in the high-pressure tank upstream from the compression chamber was around 40 bar and the initial driver gas pressure was 3 bar. The shock tube, 6.44 m long and 7 cm in diameter, has a number of flush-mounted pressure and heat flux gauges, which may be used for shock-speed determination with an error of less than 1%. For the optical experiments, it was equipped with a test chamber located 3.5 m downstream from the diaphragm. Because the facility was working as a shock generator, the shock tube was connected directly to the dump tank to avoid any reflected shocks. Special attention was given to pollution caused by impurities (metallic or hydrocarbon particles coming from the piston and the burst diaphragms from previous runs). Prior to each shot, the compression chamber and the shock tube were thoroughly cleaned with acetone and alcohol. The shock tube was then outgassed by first creating a vacuum of at least 10^{-3} mb, and second, filling it with the test gas at 10 mb; this operation was repeated at least four times for an efficient removal of the residual air molecules. To check the cleanliness of the shock tube, a shot was made in the N_2-O_2 mixture with the monochromator centered at the same wavelength as for the measurements presented here. The absence of any CN or metallic lines in this region of the spectrum proved that the flow was almost free from pollution.

Optical Setup

The optical setup is schematically presented in Fig. 3: light is collected through a vertical slit 500 μm wide, and focused onto an optical fiber bundle with a reception slit 200 μm wide. The solid angle of light collection is less than 10^{-3} sr (shown greatly exaggerated in the figure), and the spatial smearing at the center of the shock tube, which gives the temporal resolution of the measurement, is estimated to be ~0.8 mm. The optical fiber then guides the light into a Jobin–Yvon monochromator of 640 mm focal length, equipped with a holographic grating of 3000 lines per mm. Using this grating at 3872 Å results in an 85-Å-wide spectrum and a resolution better than 1.2 Å (most of the CN spectra was recorded in this configuration). For a less-dispersive spectrum measurement in the case of the Swan bands, a grating of only 600 lines was also used. The streak camera system (Hamamatsu photonics) was adapted to the monochromator by means of specially designed optics. The streak unit allows time-resolved recording of the selected band of spectrum at different time scales, from 10 ns to 50 ms; our measurements, however, were all made with an effective time scale of 16.36 μs. A pressure gauge, located 20 cm upstream from the experimental chamber, provided the triggering signal for the streak unit. The two-dimensional data are collected as a 1000 × 1018 pixels 12-bit image at the end of the streak unit on a charge-coupled device camera, cooled by Peltier effect of −30°C to reduce thermal noise.

Because the calibration of the monochromator is very sensitive to ambient temperature fluctuations, a mercury lamp was used for regularly checking the optimal arrangement. Background noise was automatically subtracted from each measurement. A shading correction was applied to compensate the spatial nonuniformity of the sensitivity of the complete streak imaging system, caused by lens aberration. Because the streak image obtained in the Titan mixture for CN emission was low in intensity, the signal-to-noise ratio (SNR) was at best 30:1 and at worst 4:1. Thus, a smoothing function[19] was applied to this streak image to improve the SNR and the quality of the spectra taken from the image at different instants. It was applied only in the temporal direction of the image because the signal was mostly deteriorated in this direction because of the time-spreading effect of the streak unit. Streak images obtained in other mixtures had better SNRs, and, therefore, did not need any filtering/smoothing process.

Table 1 Experimental conditions

	CH_4-N_2-Ar			
Conditions	1	2	CO_2-N_2	CO
p_1, mb	2.19	11.02	1.96	5.36
V, ms^{-1}	5560	5130	5800	5200

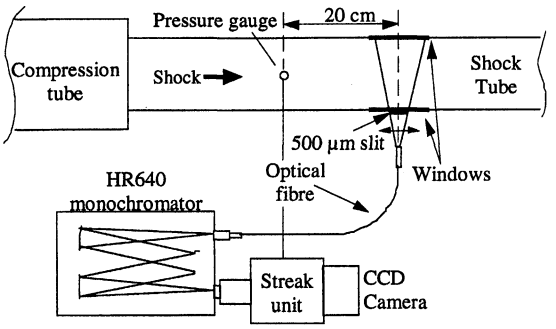

Fig. 3 Optical arrangement with streak camera.

Two series of shots were made in the CH_4-N_2-Ar mixture, one at low and one at high initial test gas pressure. The characteristic shock conditions of the shots performed in the three different mixtures are summarized in Table 1.

Results and Discussion

Typical Entry Conditions

CH_4-N_2-Ar Mixture

Figures 4a and 4b show the experimental streak image and the corresponding simulation represented in false colors for the $\Delta v = 0$ sequence of CN in the CH_4-N_2-Ar mixture at 2.19 mb initial pressure. The simulated image is calculated using the computed gasdynamic parameters given by Ref. 8 and the spectrum calculation of CN. Convolution caused by spectral slit and temporal functions are included. Figure 5b represents the recorded evolution of the emission intensity of the 0–0, 1–1, and 2–2 bands. In this figure, we may detect an oscillatory behavior of the various plotted lines. However, these oscillations differ from those presented in Ref. 5, because they are random, small, and not correlated, so that they seem to be insignificant and participate to the background noise. A broad experimental spectrum, obtained by laying several streak measurements side-by-side at different wavelengths, is shown compared with the experimental data from Park et al.[2] in Fig. 6. These results show a fair agreement with each other.

A closer analysis of the $\Delta v = 0$ sequence of CN is made, and spectra from this band, taken at three different distances from the experimental streak image, are represented in Fig. 5a. The position at maximum intensity, as mentioned in the figures, corresponds to the emission overshoot behind the shock. The time coordinate of the spectra is thus shown referenced from this point, because the exact distance between the shock layer and this overshoot could not be resolved, the triggering jitter of the streak system being between 1 and 2 μs. It may be observed, e.g., that the spectrum at the maximum intensity exhibits an anomalous behavior: the intensity of the 1–1 vibrational band is relatively high compared to the 0–0 band.

The vibrational population distribution (normalized with respect to the population of the level $v = 0$), deduced from the

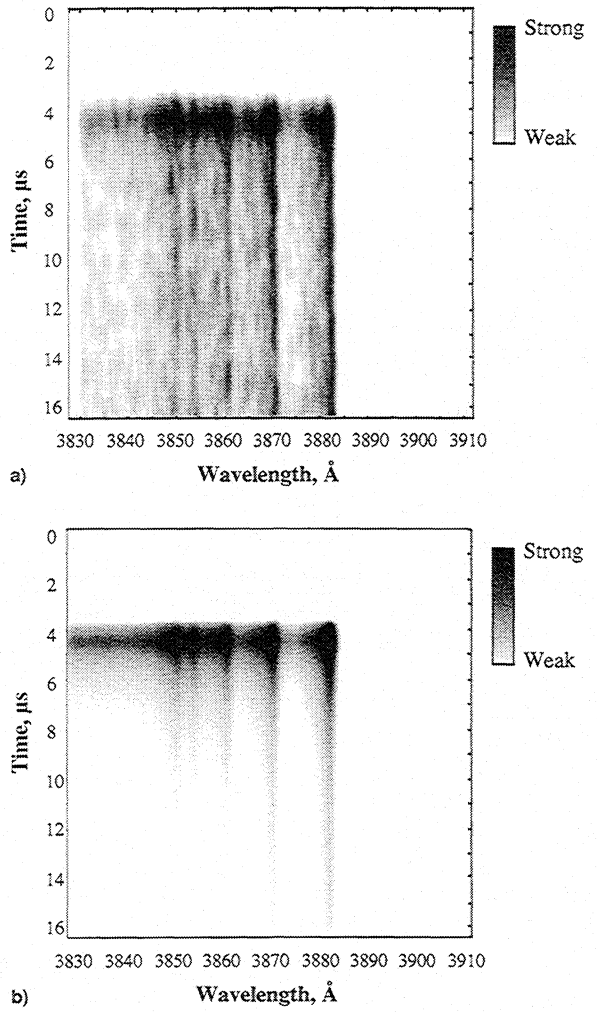

Fig. 4 Streak images in the CH_4-N_2-Ar mixture for p_1 = 2.19 mb and V = 5560 m/s: a) experimental recording and b) numerical simulation.

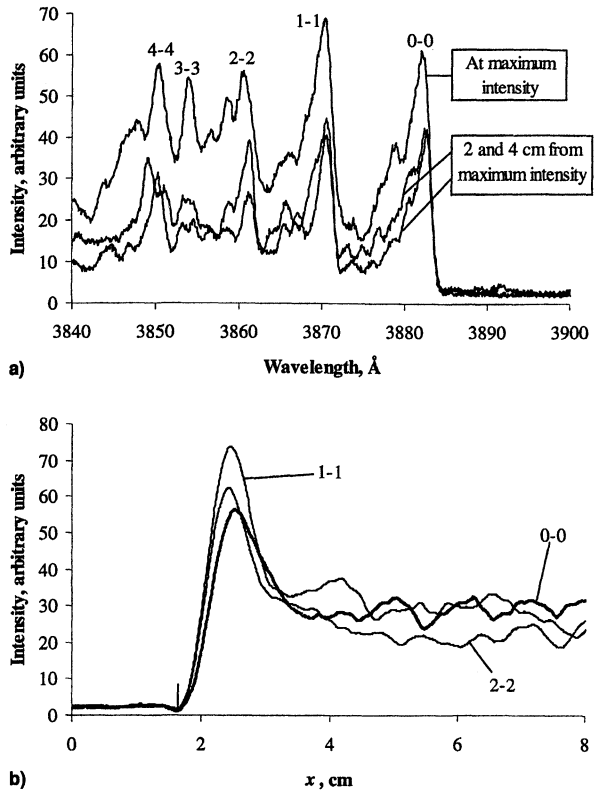

Fig. 5 Profiles taken from the experimentally recorded streak image in the CH_4-N_2-Ar mixture for p_1 = 2.19 mb and V = 5560 m/s: a) spectra at three different time coordinates behind the shock and b) time evolution of the intensities of the 0–0, 1–1, and 2–2 vibrational bands.

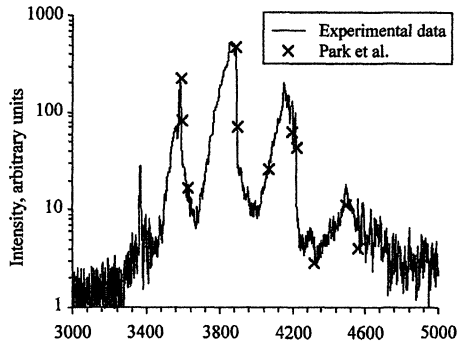

Fig. 6 Comparison between the experimental integrated spectrum from the present work and some experimental data points from Park et al.[2] for a shock wave in the CH_4-N_2-Ar mixture.

spectra measured in the CH_4-N_2-Ar mixture in the low-pressure condition, is represented by Fig. 7a. The atypical aspect of the spectrum taken near the shock is confirmed by this calculation as being a result of the overpopulation of the vibrational levels v = 1 and 2. Some evidence of an overpopulation of v = 6 can also be noticed. However, farther downstream, this phenomenon disappears and the vibrational population relaxes toward a Boltzmann distribution. The vibrational temperatures deduced from these data are shown in Fig. 8. Apart from the region estimated to be less than x = 5 mm, where a non-Boltzmann vibrational population is observed, the experimental vibrational temperature evolution shows a behavior similar to the one obtained by numerical analysis. However, these results are quantitatively rather different from each other (15–25% difference). A spectrum taken at x = 41.3 mm from the maximum intensity is compared with a numerical simulation in Fig. 9. The vibrational temperature corresponding to this spectrum is equal to 9300 ± 500 K and, within experimental error, agrees with the numerical result.

CO_2-N_2 Mixture

In the CO_2-N_2 mixture, the recording of the Δv = 0 band of CN was done at 1.96-mb initial pressure and a shock speed of 5800 ms^{-1}. The relative vibrational population density calculated from the experimentally recorded spectra exhibits Boltzmann trends. From these distributions, the vibrational temperature evolution is calculated and plotted as a function of distance behind the shock in Fig. 10, the average error on these data being ~500 K. The comparison with the experimental vibrational temperatures and a numerical computation from Ref. 9 shows a fair agreement. It should be pointed out that in this mixture the non-Boltzmann behavior of CN, as observed in the Titan mixture, does not occur at all.

High-Pressure Condition

To study the influence of the initial conditions on the spontaneous emission of CN, a recording of the Δv = 0 band of this radical was done at a higher initial pressure (11.02 mb) and a shock speed of 5130 ms^{-1} in the CH_4-N_2-Ar mixture, this speed remaining close to the one at low pressure. The vibrational population distribution for the vibrational levels higher than v = 5 (Fig. 7b) shows a very marked deviation from a Boltzmann distribution, over the entire observed distance of 4.3 cm, from the maximum intensity layer. It should be noted that over this distance, the features of the spectrum

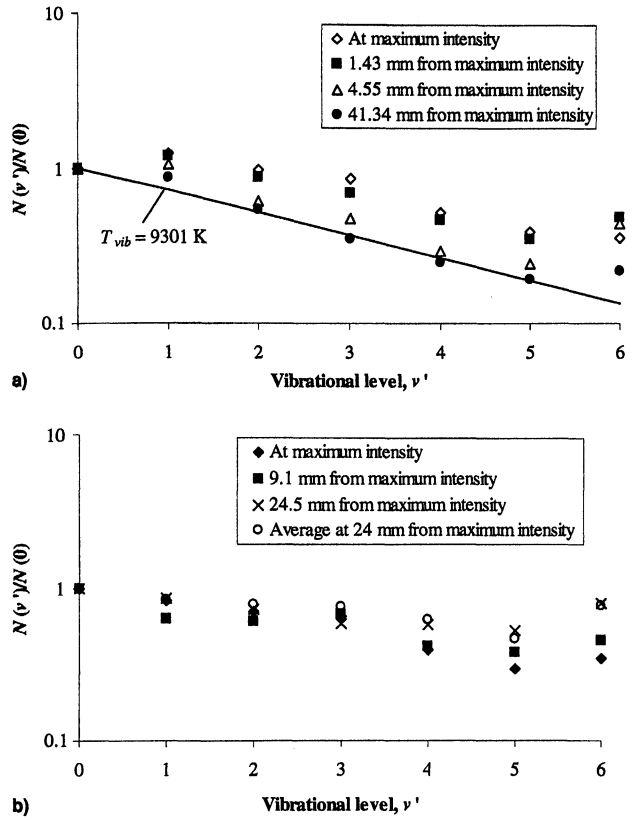

Fig. 7 Experimental vibrational population distribution at different instants behind shocks in the CH_4-N_2-Ar mixture: a) p_1 = 2.19 mb, V = 5560 m/s and b) p_1 = 11.02 mb, V = 5130 m/s.

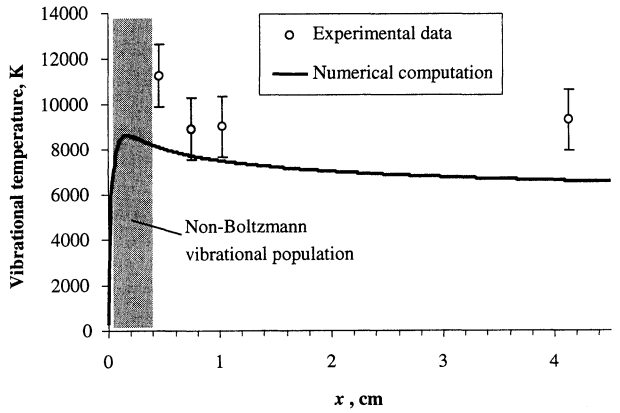

Fig. 8 Evolution of vibrational temperature behind a shock in the CH_4-N_2-Ar mixture for p_1 = 11.02 mb and V = 5560 m/s.

as well as its intensity only slightly vary, resulting in no clear overshoot (Figs. 11a and 11b). Although in these conditions the intensity of the $\Delta v = 0$ band rapidly reaches a constant value downstream from the shock, the vibrational population remains highly excited, indicating a state of vibrational nonequilibrium. The experimental evolution of the intensity of the $\Delta v = 0$ band shows a strong disagreement with the corresponding numerical analysis.

Pure CO

The C_2 bands measured in pure CO are shown in Figs. 12a and 12b. The radiation coming from the $\Delta v = 0$ and $\Delta v = +1$ sequences of the Swan bands has been integrated and compared with the corresponding simulation: a fair agreement may be observed between both results. The spectrum over this region has been determined using the variables obtained

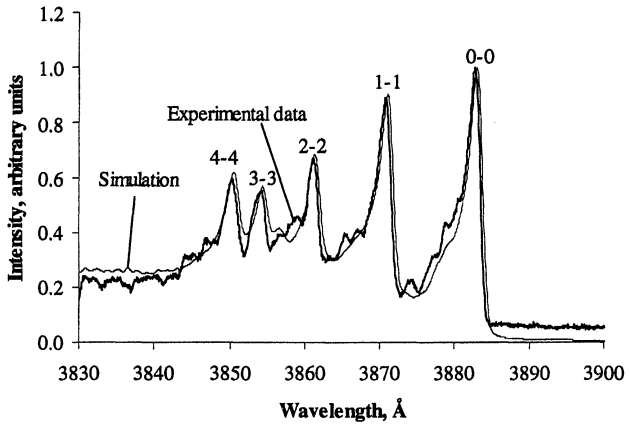

Fig. 9 Experimental and calculated spectra of CN in CH_4-N_2-Ar for T_{rot} = 8000 K and T_{vib} = 9300 K.

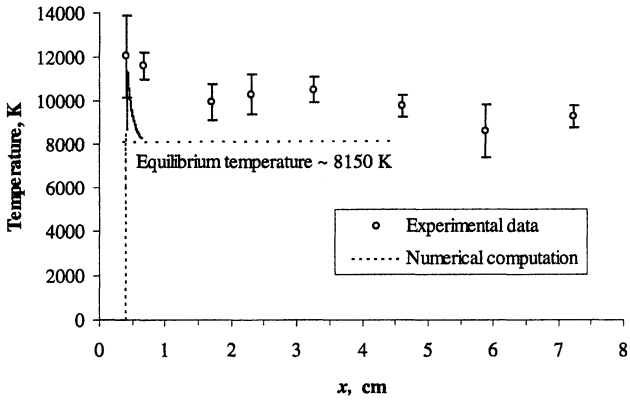

Fig. 10 Evolution of vibrational temperature behind a shock in the CO_2-N_2 mixture for p_1 = 1.96 mb and V = 5800 m/s.

from the numerical computation behind a shock wave in this gas.

Analysis

The results of the experiments carried out in the CH_4-N_2-Ar mixture at typical low initial pressure conditions are more or less consistent with a classical numerical computation using a three-temperature kinetic model. Moreover, these results seem to agree with previous experimentation from Refs. 2 and 3. However, time-resolved spectra of CN measured behind the shock have revealed a short region in the vicinity of the shock layer where this radical is vibrationally excited. This state results in a non-Boltzmann distribution in the vibrational energy levels of CN. In the experiments made at higher initial pressure, this phenomenon becomes important and lasts for a long period of time. These experimental conditions have not been investigated by previous authors and the reason for the anomalous behavior of CN is unknown. Under very different experimental conditions, observation of deviation from a Boltzmann distribution in the vibrational population of CN, formed in a corona discharge of expanding acetonitrile, has also been reported by Rehfuss et al.,[13] particularly from levels higher than $v = 5$. From our results, we may observe that the vibrational relaxation of CN is also complex in nature. We may reasonably conclude that its atypical behavior at high initial pressure conditions should be further studied, and if necessary, should be taken into account in the chemical model of the CH_4-N_2-Ar mixture. Observation of the other bands of CN, such as the $\Delta v = +1$ band, should also give more information on the vibrational relaxation of CN.

From a practical point of view, however, this present work does not give a quantitative evaluation of the effect of the non-

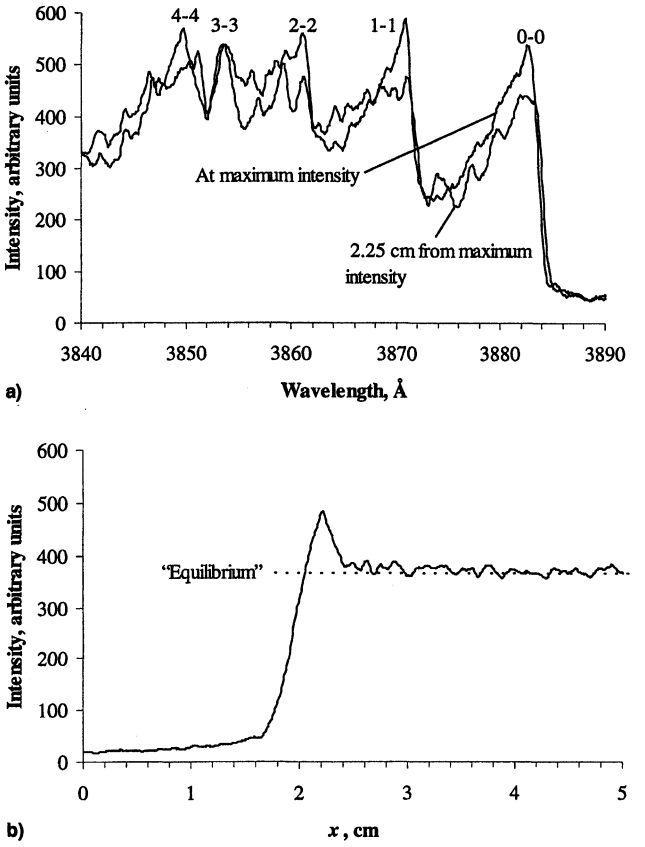

Fig. 11 Profiles taken from the experimentally recorded streak image in the CH_4-N_2-Ar mixture for p_1 = 11.02 mb and V = 5130 m/s: a) spectra at two different instants behind the shock and b) time evolution of the integrated intensity of the $\Delta v = 0$ band of CN.

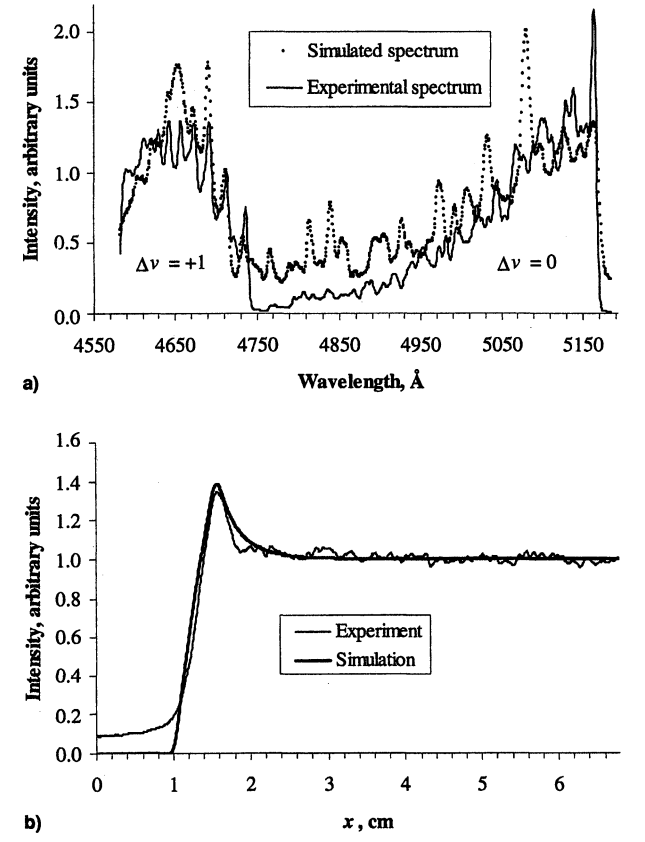

Fig. 12 C_2 Swan bands in pure CO for p_1 = 5.36 mb and V = 5200 m/s: a) spectra and b) integrated intensity evolution of the $\Delta v = 0$ and $\Delta v = +1$ sequences behind the shock.

Boltzmann behavior of CN on the total heat flux during a Titan entry phase (if such pressure conditions should prevail). This aspect of the study remains an open question and still needs to be investigated in depth.

Conclusions

The experimental study of time-resolved spectra of the $\Delta v = 0$ band of CN in the CH_4-N_2-Ar and CO_2-N_2 mixtures at typical entry conditions qualitatively confirms the results predicted by numerical codes. However, evidence of non-Boltzmann distributions in the vibrational population of the $B^2\Sigma^+$ electronic state of CN has been observed. This phenomenon seems to occur in a short distance behind shocks at low initial pressure, and for a longer distance behind shocks at high initial pressure. In shocks in the CO_2-N_2 mixture, spectrum recordings show that the vibrational relaxation of CN seems to go through simpler phases and reaches a Boltzmann distribution very rapidly. However, shots at high initial pressure remain to be done and require further investigation. The $\Delta v = 0$ and $\Delta v = +1$ bands of the C_2 Swan system have also been observed, and the obtained results agree with numerical simulations of the radiation emitted from shocks in CO gas.

References

[1]Keck, J. C., Camm, J. C., Kivel, B., and Wentink, T., Jr., "Radiation from Hot Air. Part II: Shock Tube Study of Absolute Intensities," *Annals of Physics*, Vol. 7, No. 1, 1959, pp. 1–38.

[2]Park, C. S., Bershader, D., and Park, C., "Radiative Emission from Stimulated Shock Layer of the Huygens Probe," *Journal of Thermophysics and Heat Transfer*, Vol. 10, No. 4, 1996, pp. 563–569.

[3]Labracherie, L., "Détermination des Températures Rotationnelles et Vibrationnelles de CN à l'Aval d'un Choc Droit se Propageant dans une Atmosphère de Titan Reconstituée," PhD. Dissertation, Univ. de Provence, Marseille, France, 1994.

[4]Baillon, M., Taquin, G., and Soler, J., "Huygens Probe Radiative Environment," *Proceedings of the 19th International Symposium on Shock Waves*, Vol. 2, Springer–Verlag, Berlin, 1995, pp. 339–346.

[5]Morioka, T., Sakurai, N., Maeno, K., and Honma, H., "A Shock Tube Study on Nonequilibrium Shock Front Radiation in Low-Density Air," *Proceedings of the 21st International Symposium on Shock Waves*, Paper 3713, 1997.

[6]Nelson, H. F., Park, C., and Whiting, E. E., "Titan Atmospheric Composition by Hypervelocity Shock Layer Analysis," *Journal of Thermophysics and Heat Transfer*, Vol. 5, No. 2, 1991, pp. 157–165.

[7]Park, C., Howe, J. T., and Jaffe, R. L., "Review of Chemical-Kinetics Problems of Future NASA Missions, 2: Mars Entries." *Journal of Thermophysics and Heat Transfer*, Vol. 8, No. 1, 1994, pp. 9–23.

[8]Koffi-Kpante, K., "Etude des Phénomènes de Désèquilibre Thermochimique dans la Couche de Choc Radiative de l'Atmosphère Simulée de Titan," Ph.D. Dissertation, Univ. de Provence, Marseille, France, 1996.

[9]Mazoué, F., "Analyse de la Couche de Choc dans le CO_2. Application à l'Entrée Atmosphérique de la Planète Mars," Ph.D. Dissertation, Univ. de Provence, Marseille, France, 1994.

[10]Hanson, R. K., "Shock-Tube Study of Carbon Monoxide Dissociation Kinetics," *Journal of Chemical Physics*, Vol. 60, No. 12, 1974, pp. 4970–4976.

[11]Appleton, J. P., Steinberg, M., and Liquornik, D. J., "Shock-Tube Study of Carbon Monoxide Dissociation Using Vacuum-Ultraviolet Absorption," *Journal of Chemical Physics*, Vol. 52, No. 5, 1970, pp. 2205–2221.

[12]Engleman, R., "The $\Delta v = 0$ and +1 Sequence Bands of the CN Violet System Observed During the Flash Photolysis of BrCN," *Journal of Molecular Spectroscopy*, Vol. 49, No. 1, 1974, pp. 106–116.

[13]Rehfuss, B. D., Suh, M.-H., and Miller, T. A., "Fourier Transform UV, Visible, and Infrared Spectra of Supersonically Cooled CN Radical," *Journal of Molecular Spectroscopy*, Vol. 151, No. 2, 1992, pp. 437–458.

[14]Huber, K. P., and Herzberg, G., *Molecular Spectra and Molecular Structure: IV. Constants of Diatomic Molecules*, Van Nostrand, New York, 1979, pp. 112–114.

[15]Herzberg, G., *Molecular Spectra and Molecular Structure: I.*

Spectra of Diatomic Molecules, Van Nostrand, New York, 1966, pp. 1–280.

[16]Spindler, R. J., "Franck-Condon Factors Based on RKR Potentials with Applications to Radiative Absorption Coefficients," *Journal of Quantitative Spectroscopy and Radiative Transfer*, Vol. 5, No. 1, 1965, pp. 165–204.

[17]Arnold, J. O., Whiting, E. E., and Lyle, G. C., "Line by Line Calculation of Spectra from Diatomic Molecules and Atoms Assuming a Voigt Line Profile," *Journal of Quantitative Spectroscopy and Radiative Transfer*, Vol. 9, No. 4, 1969, pp. 775–798.

[18]Brun, R., Burtschell, Y., Chaix, A., Druguet, M.-Cl., Dumitrescu, L.-Z., Dumitrescu, M.-P., Martin, R., and Zeitoun, D., "Flow in the TCM2-Marseille Hypersonic Facility: Some New Experimental Results," *Proceedings of the 20th Symposium on Shock Waves*, World Scientific, Singapore, 1996, pp. 227–232.

[19]Press, W. H., Flannery, B. P., Teukolsky, S. A., and Vetterling, W. T., *Numerical Recipes in Fortran*, Cambridge Univ. Press, Cambridge, England, UK, 1993.